Decay of density fluctuations in gels

James E. Martin, Jess Wilcoxon, and Judy Odinek
Sandia National Laboratories, Albuquerque, New Mexico 87185
(Received 6 August 1990)

Near the sol-gel transition, gelling systems exhibit an extremely slow relaxation of thermally driven density fluctuations. We have made a detailed quasielastic light scattering study of the decay of density fluctuations in reacting silica sol-gels in the pre- and post-gel regimes, and at the gel point. In the pre-gel regime the dynamic structure factor $S(q,t)$ for the branched polymer melt has a stretched exponential tail whose characteristic time diverges at the gel point. This *critical slowing down* is due to the divergence of the average cluster size and is distinct from the usual critical slowing down observed in second-order thermodynamic phase transitions, since the initial decay rate of $S(q,t)$ is nondivergent at the gel point. In fact, at the gel point, $S(q,t)$ becomes a power law, indicating a fractal time set in the scattered field. These observations are accounted for by considering the dynamics of percolation clusters, and in this connection the analogy to viscoelasticity is described. Beyond the gel point $S(q,t)$ remains a power law, but the amplitude of the relaxing part of the intensity autocorrelation function diminishes. Finally, the dynamics of clusters diluted from the reaction bath is studied, and a crossover from power law to stretched exponential decay of $S(q,t)$ is observed. It is shown that at infinite dilution the long-time tail of the correlation function describes the internal modes of a single percolation cluster.

I. INTRODUCTION

When a solution containing a multifunctional monomer reacts to form a gel, a rich variety of structural and dynamical transformations takes place. These transformations are extraordinary in the vicinity of the sol-gel transition, where a complex viscoelastic intermediate between a liquid and solid is formed. Structural studies of branched polymers formed near the gel point demonstrate that gelation is reasonably well described by the percolation model, so it is appropriate to think of the sol-gel transition as a geometrical realization of a critical point, with the usual scaling laws in force. However, the sol-gel transition does not have *all* the characteristics of a thermodynamic critical point, since it is the connectivity correlation length that diverges, not the spatial correlation length. Thus critical opalescence does not appear at the gel point and there is no critical slowing down in the usual sense.

Nonetheless, the divergent connectivity in sol-gels imposes a severe dynamical constraint that gives rise to a novel form of critical slowing down that is microscopically manifested in the relaxation of density fluctuations,[1,2] and macroscopically manifested through stress or strain relaxation.[3–5] In either case, relaxation functions decay as power laws in time, and characteristic time scales diverge. When the sol-gel is exactly at the gel point, an exotic state of matter is obtained—a *dynamically* self-similar fluid with no associated time scale. As we shall see, photons scattered from this fluid break time itself into a fractal set. In this paper we report quasielastic light scattering investigations of the relaxation of thermally induced density fluctuations in gels, and present a dynamic scaling description of these phenomena. Our observations are compared to qualitatively similar viscoelastic studies.

In quasielastic light scattering[6] (QELS) the relaxation of density fluctuations of wave vector q is probed by measuring the autocorrelation function of the scattered intensity, $I(q,t)=\langle I(0)I(t)\rangle$ [in terms of the wavelength of light in the scattering medium λ, and the scattering angle θ, $q=4\pi\sin(\theta/2)/\lambda$]. In our first QELS measurements on sol-gels[1] we investigated the dynamics in the pre-gel regime and at the gel point. Specifically, we reported the stretched exponential time decay of $I(q,t)$ before the gel point, the power-law time decay of $I(q,t)$ at the gel point, and the divergence of both the arithmetic average and "typical" relaxation times. These measurements are elaborated here, and new results are presented for the dynamics of the post-gel regime, and for the dynamics of semidilute and dilute branched polymer solutions, obtained by diluting a sol-gel near the gel point.

In the post-gel regime a power-law correlation function is found whose amplitude diminishes as the modulus of the gel increases. In semidilute branched polymer solutions, correlation functions are found that cannot be described by a single time scale; rather, the initial decay rate is proportional to q^2, whereas the long-time tail is a stretched exponential $\exp[-(t/\tau)^{\beta}]$ with a decay rate τ^{-1} that is roughly q^3 dependent. However, in dilute solutions the correlations functions are described by a single time scale that is $1/q^3$ dependent in the regime where $qR \gg 1$, and the correlation functions are no longer stretched exponentials.

II. EXPERIMENT

Silica gels were prepared in methanol from $1.0M$ tetramethoxysilicon (TMOS), $4.0M$ H_2O, and $0.1M$

NH_3OH base catalyst. To avoid dust contamination, preparation was conducted in a clean bench, and the final solutions were either filtered with 0.2-μm polytetrafluoroethylene (PTFE) filters into scattering cells, or centrifuged for 15 min at 30 000 g. QELS measurements were made in the *homodyne* (self-beating) mode with an argon-ion laser at $\lambda=457.9$ nm, and a 256-channel correlator. Near the gel point, autocorrelation functions were collected over an extensive relaxation time regime by running at three delay times, 3.6×10^{-7}, 2.0×10^{-5}, and 1.3×10^{-3} sec, and then merging the three pieces by appropriate normalization in the two overlap regimes. Autocorrelation function merging with the delay times 1.0×10^{-6} and 1.0×10^{-4} sec was used to integrate $I(q,t)$ to obtain the average relaxation time. This integration was performed numerically, without recourse to curve fitting techniques. In all cases the homodyne dynamic structure factor $S(q,t)$ was obtained by subtracting the *calculated* incoherent base line from $I(q,t)$ and normalizing to unity at $t=0$. With such slowly relaxing samples it is not possible to use the delay channels to estimate the true base line near the gel point, so this is one case where immaculately dust free samples are essential. Gel points were determined by attempting to dilute aliquots of the reacting mixture—the gel point was taken to be the midpoint of the time interval between the last soluble sample and the first insoluble sample.

III. THE REACTION BATH

A. Approach to the gel point

Before discussing the quasielastic scattering from silica sol-gels, it is helpful to have an overview of the growth and structure that precedes the gel point. Experiments show that growth is described by aggregation until clusters overlap, at which point growth proceeds via a percolative transition.[7] In the following, these stages are discussed in more detail.

When a base catalyst is added to a tetramethoxysilicon solution, the methoxy groups are hydrolyzed to produce various silicic acids that then condense to form dimers, trimers, etc. and eventually a gel. At the very earliest times both the kinetics of growth and the structure of the polycondensates are nonuniversal, being highly dependent on such factors as pH, amount of added salt, etc. This growth regime is not well understood, but it is likely that the supersaturation of silicic acids leads to a nucleation event with monomers accreting onto nascent clusters. In any case, it is known that objects of a relatively high apparent fractal dimension are formed in this stage. However, at a radius of about 10 nm a crossover is observed to exponential growth, Fig. 1, that is indicative of *reaction-limited* cluster-cluster aggregation.[8,9] Since the isoelectric point of silica polycondensates is in the range of pH 2–3, at high pH the silicic acid groups are dissociated, leaving a negatively charged polycondensate with a double layer. The resultant screened Coulomb interaction makes the probability of a collision between aggregates small, leading to reaction-limited growth kinetics. However, if the Coulomb interactions are screened by adding a uni-univalent salt such as NaCl, the rate of

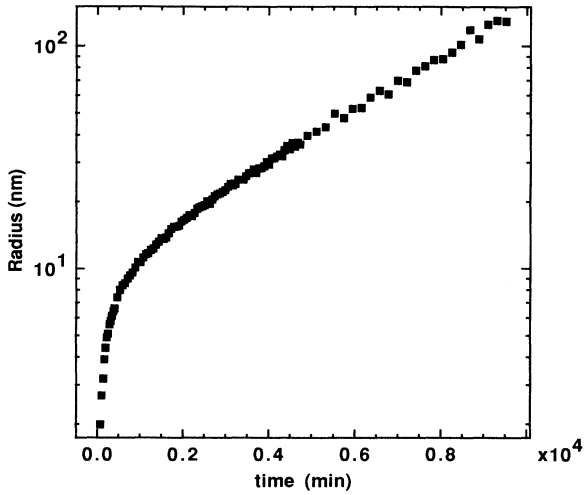

FIG. 1. After an initial phase of growth that appears to be due to colloid formation, the hydrodynamic radius of the base-catalyzed silica clusters grows exponentially with time, indicating reaction-limited cluster-cluster aggregation. The sample composition was 0.1M TMOS, 2.2M H_2O, catalyzed with 0.0044M NH_4OH and 0.002M NaCl at 30° C.

aggregation increases by many orders of magnitude, and the power-law growth associated with diffusion-limited aggregation is observed,[8,10] as in Fig. 2. In the limit of low salt and high pH, where the growth is exceedingly slow due to pronounced Coulomb interactions, it is even possible to form aggregates with a fractal dimension approaching 1, in accord with recent simulations[11] of reaction-limited aggregation in $1/r^{\epsilon}$ potentials.

The nonequilibrium aggregation stage eventually crosses over to the critical growth associated with gela-

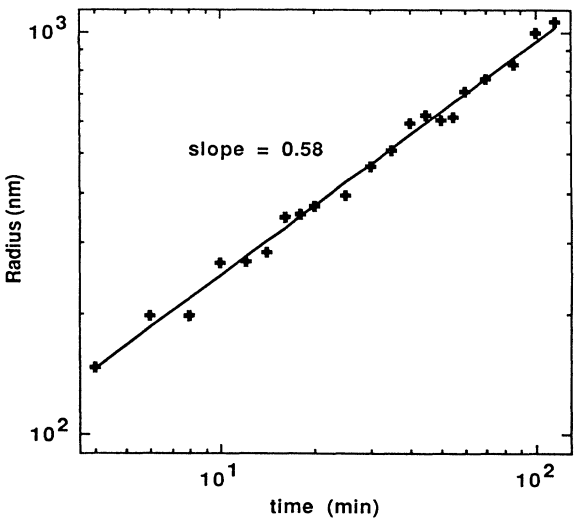

FIG. 2. Under aggressive reaction conditions power-law growth $R\sim t^{0.58}$ of silica clusters is observed, indicating diffusion-limited cluster-cluster aggregation. The sample composition was 0.001M TMOS, 30M H_2O, catalyzed with 0.04M NH_4OH and 1.0M NaCl at 30 °C.

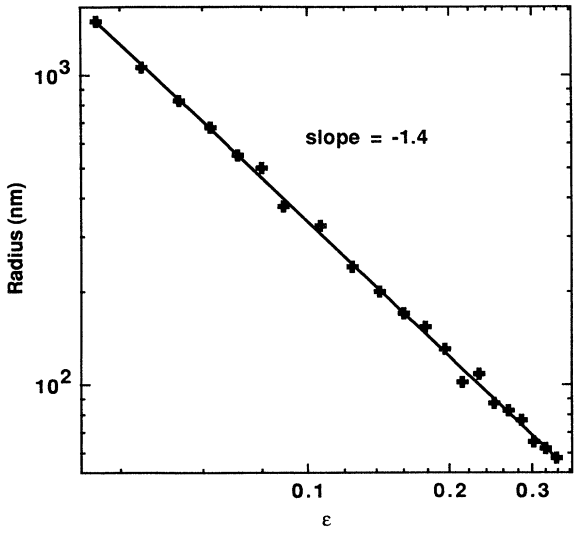

FIG. 3. The z-average hydrodynamic radius for a base-catalyzed TMOS gel diverges as $R_z \sim \epsilon^{-1.35}$ (exponent uncorrected for swelling). This is in reasonable agreement with the swollen percolation prediction of $R_z \sim \epsilon^{-1.1}$. Here ϵ is the reduced time from the gel point.

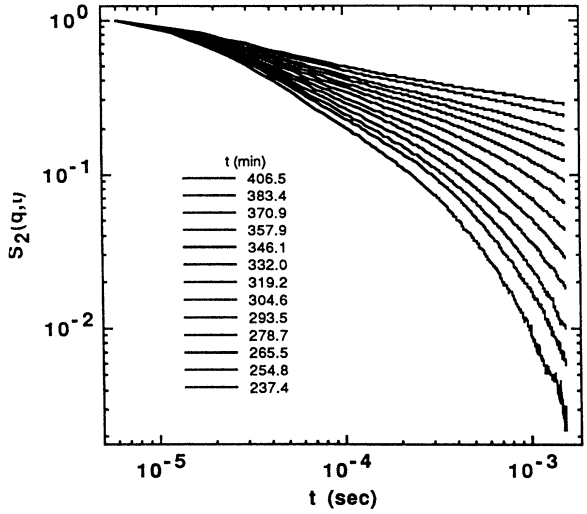

FIG. 4. Homodyne correlation functions are logarithmically plotted for a gelling base-catalyzed tetramethoxysilicon solution with the top curve at the gel point of ~406 min. As the gel point is approached, a pronounced slowing down of the relaxation is observed, until at the gel point an ultraslow power-law decay becomes evident.

tion,[12] Fig. 3, when the aggregates become sufficiently large to fill the volume of the solution. This will occur when the intrinsic viscosity $[\eta]$ of the aggregates reaches c^{-1} where c is the concentration of silica in the solution. Since the intrinsic viscosity is proportional to the mean cluster specific volume R^{d-D}, where R is the mean aggregate radius, d is the dimension of space, and D is the fractal dimension, this crossover occurs when the mean radius is $\sim c^{-1/(d-D)}$. Thus at low concentrations of silica, large clusters are formed by nonequilibrium aggregation processes. Since we are interested in the dynamics of the sol-gel transition, we chose to work at high silica concentrations where the aggregation-gelation crossover occurs at small cluster sizes, far from the gel point. Given this rudimentary description of the pre-gel regime, we now present the phenomenology of the dynamics of the sol-gel transition.

As the gel point is approached, correlation functions become progressively more nonexponential, indicating an increasingly broad spectrum of relaxation times.[1,2] The homodyne autocorrelation functions in Fig. 4, taken at roughly 10 min intervals prior to the sol-gel transition, demonstrate this point and further indicate an approach to power-law decay at the gel point ($t_{\rm gel} \sim 406$ min). However, the decay in the pre-gel regime is more rapid than a power law, the long-time tail being well described as a "stretched" exponential decay, $S_2(q,t) \sim \exp[-(t/\tau_z)^b]$ with $b = 0.66 \pm 0.05$, as shown in Fig. 5. These data indicate that near the gel point the correlation function is a power-law decay that is truncated by a stretched exponential tail. (This general type of behavior is observed in spin glasses, due to the percolative structure of a random alloy.)

As the gel point is approached, certain characteristic relaxation times diverge, indicating that a form of critical slowing down occurs at the gel point. In fact, it is possible to define several characteristic times that behave quite differently as the gel point is approached. For example, the critical plot in Fig. 6 of the relaxation time τ_z of the stretched exponential tails in Fig. 5 indicates the divergence $\tau_z \sim \epsilon^{-2.5 \pm 0.1}$ where $\epsilon = |t_{\rm gel} - t|/t_{\rm gel}$ (we will later show that this is the longest characteristic time in the system). The arithmetic mean relaxation time $\langle \tau \rangle$, ob-

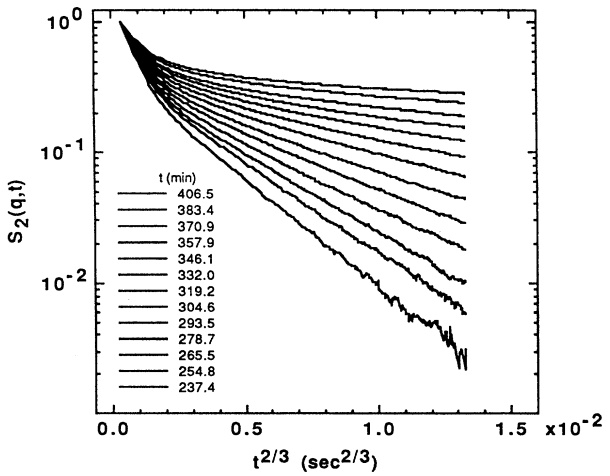

FIG. 5. The long-time tail of the correlation functions shown in Fig. 4 are shown to be described by the stretched exponential $\exp[-(t/\tau_z)^{-0.65 \pm 0.05}]$ for $t > \tau_z$, where τ_z is a decay time associated with a typical cluster. The top curve is closest to the gel time of about 406 min.

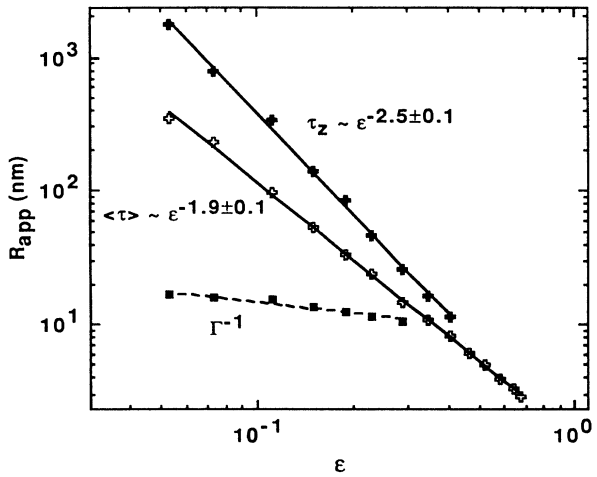

FIG. 6. As the silica solutions approach the gel point, some characteristic times of the decay diverge, indicating critical slowing down. The arithmetic average relaxation time, obtained as the integral of the correlation function, shows the power-law divergence $\langle\tau\rangle \sim \epsilon^{-1.9\pm0.1}$, where $\epsilon = |t_{gel} - t|/t_{gel}$, whereas the slowest decay time, obtained from the stretched exponential tails in Fig. 5, scales like $\tau_z \sim \epsilon^{-2.5\pm0.1}$. The inverse first cumulant Γ^{-1} does not diverge. To remove the q dependence, these decay times are plotted as dynamic correlation lengths $R_{app} \equiv (k_B T/6\pi\eta_0)q^2\langle\tau\rangle$.

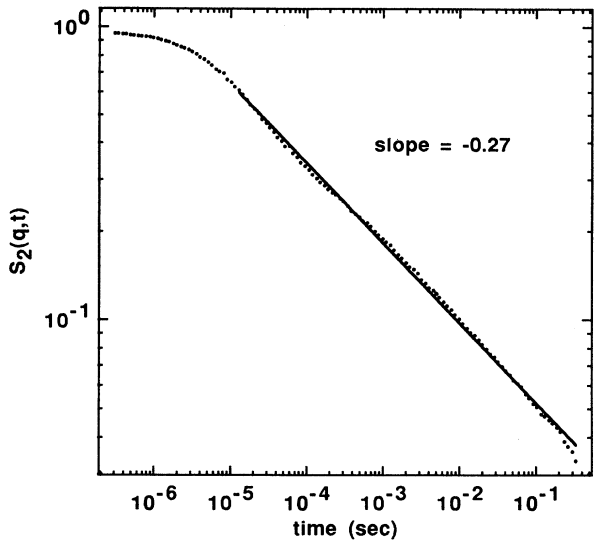

FIG. 7. At the gel point, the homodyne correlation function of a tetramethoxysilicon gel shows a power-law decay over five decades in time at $q^{-1} = 29.7$ nm. The curvature at $t < 3$ μsec is apparently due to cooperative diffusion, the fastest observable relaxation process in the system. It is noteworthy that the initial decay rate is finite, although the average relaxation time has diverged at this point.

tained by numerically integrating $S(q,t)$ over a 4.4 decade time domain, has a somewhat weaker divergence, with $\langle\tau\rangle \sim \epsilon^{-1.9\pm0.1}$. In contrast, the *harmonic* mean $\langle\tau^{-1}\rangle^{-1}$ of the relaxation time spectrum, obtained from the initial relaxation rate $\Gamma = -d\ln S(q,t)/dt|_{t=0}$, does not diverge since this average is sensitive only to the most rapid decay processes in the system. Thus the critical dynamics observed near the sol-gel transition is qualitatively unlike that observed for thermodynamic phase transitions, where there is only a single characteristic time and both $\langle\tau\rangle$ and $\langle\tau^{-1}\rangle^{-1}$ diverge with the same power of ϵ.

B. The gel point

For a system that exhibits critical slowing down it is possible to conceive of two simple descriptions of relaxation phenomena at the critical point. First, the decay can be described by a function $f(t/\tau)$ that is scaled by a single divergent characteristic time τ, so that there is simply *no* relaxation at the critical point. This is precisely the description of critical slowing down in second-order phase transitions,[13] where $f(t/\tau) = e^{-t/\tau}$. Second, the observed relaxations can be *independent* of the divergent characteristic time, at least on times short compared to this time. This is possible if the decay is described by a function that does not contain a time scale—a power law. In this case, relaxation can still occur, even though the average relaxation time is infinite. In the following, we demonstrate that the sol-gel transition falls into this latter class.

A correlation function for a base-catalyzed $1.0M$ TMOS solution at the gel point, shown in Fig. 7, demonstrates an initial exponential decay followed by ~5 decades of power-law decay with $S_2(q,t) \sim t^{-0.27\pm0.03}$. The initial exponential relaxation is probably due to cooperative diffusion, and merely indicates a short-time cutoff in the infinitely wide spectrum of relaxation times. In order to explore the universality of the decay exponent, a $1.0M$ TMOS gel was made using a two-step catalysis scheme wherein the hydrolysis of the methoxy groups was catalyzed with acid and the condensation reaction to make bridging Si—O—Si bonds was catalyzed with base: this gel gave the same decay exponent, within experimental error. A base-catalyzed $0.25M$ TMOS gel also gave similar results, indicating that the decay exponent is insensitive to preparative methods if the spatial correlation length of the gelling solution is much smaller than the reciprocal scattering wave vector.

The power-law decay observed at the gel point is an interesting physical realization of *fractal time,* a subject originally discussed by Mandelbrot[14] in connection with the occurrence of transmission errors in data streams. The intensity autocorrelation function is just the density-density correlation function $\langle\rho(0)\rho(t)\rangle$ of detected photons, since the intensity is the number of detected photons per unit time. Thus the detected photons form a disconnected fractal dust on the time axis, with a fractal dimension less than 1. Since in general the density-density correlation function of a fractal is the power law $\langle\rho(0)\rho(r)\rangle \sim 1/r^{d-D}$, by observing that the dimension of time is $d = 1$ a fractal time set of detected photons should give the decay $S_2(q,t) \sim 1/t^{1-D_p}$. The fractal dimension of the detected photons scattered from the critical gel is thus $D_p = 1 - 0.27 = 0.73$. Just as a mass fractal has no internal characteristic length, fractal time lacks an inter-

nal characteristic time, as evidenced by the divergent times we observe.

To obtain a better understanding of the gel point dynamics we made a base-catalyzed 0.25M TMOS gel with a gel time of ~37 days, in order to have sufficient time in the vicinity of the gel point to study the q dependence of the correlation function. After collecting correlation functions in the range 29.7 nm $< q^{-1} <$ 143 nm, we noticed that on the largest length scales the correlation function seemed to clearly indicate the presence of two separate decay processes—an exponential decay at short times that crosses over to a power-law tail at long times, as shown in Fig. 8. On smaller length scales (large q) this crossover is not as evident since the amplitude of the exponential contribution decreases. To separate the initial exponential contribution from the power-law tail we used a dynamic structure factor of the form

$$S(q,t) = Ae^{-\Gamma t} + \frac{(1-A)}{(1+t/\tau)^{D_p/2}}, \quad (1)$$

where A is an amplitude, Γ is the relaxation rate associated with the exponential decay, τ is the time at which the power-law tail begins, and D_p is the fractal dimension of the set of scattered photons. The factor of 2 on the exponent D_p occurs because the correlated part of the intensity autocorrelation function is proportional to the square of the dynamic structure factor [in practice the square of Eq. (1) was fit to the homodyne correlation function with the calculated base line subtracted]. Although the detailed form of the second term in Eq. (1) is arbitrary, this function gives an excellent fit to the data, as shown by the small, nonsystematic residuals in Fig. 8.

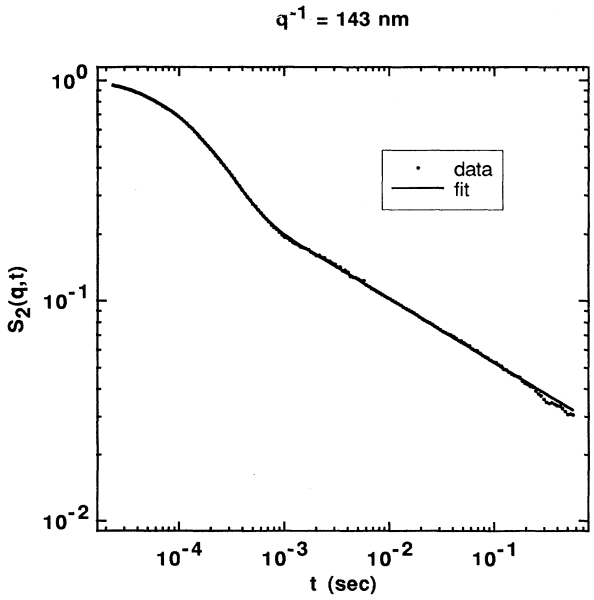

FIG. 8. A homodyne correlation function for a 0.25M base-catalyzed TMOS gel taken at a relatively long length scale of 143 nm shows a pronounced exponential decay followed by a power-law tail with an exponent of ~0.3. The fit to the square of Eq. (1) is very good, as indicated by the small residuals.

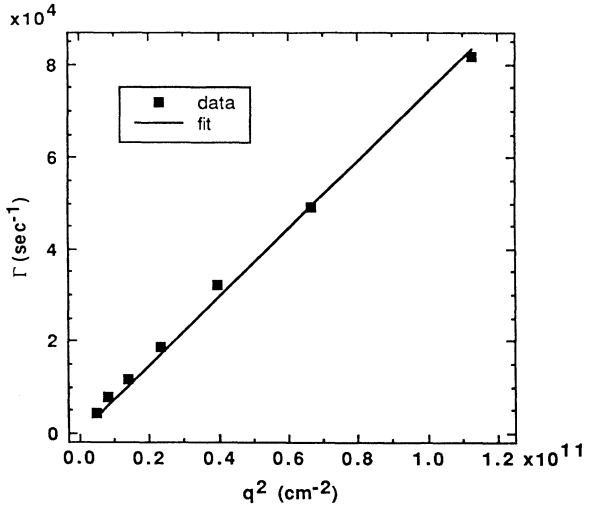

FIG. 9. The initial decay rate for correlation functions at the gel point is shown to be q^2 dependent. These data were taken from a 0.25M base-catalyzed TMOS gel that gelled in ~37 days. Due to the long gel time it was possible to investigate the angular dependence of the correlation functions without a substantial change in the properties of the gel.

And since the data span 4 decades of time, convergence in the nonlinear least squares fitting process was good, yielding unambiguous parameters.

The time scales obtained from the gel point correlation functions appear to be $1/q^2$ dependent, indicating that in

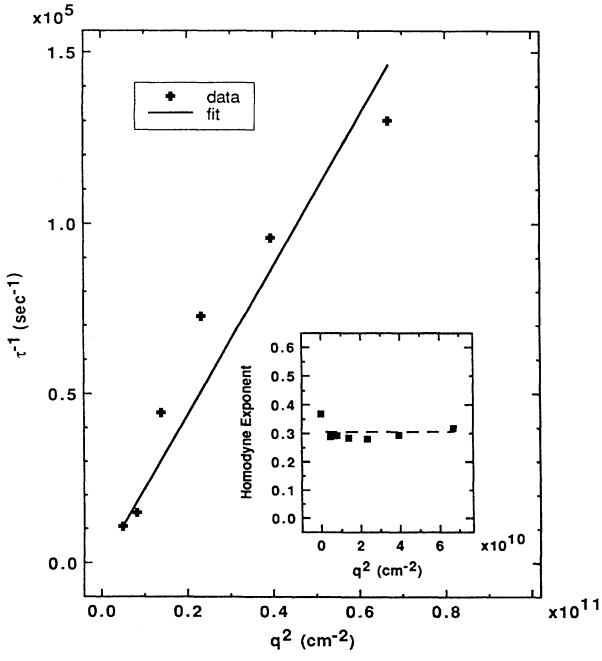

FIG. 10. The short-time cutoff of the power-law tail, obtained by fitting Eq. (1) to gel point correlation functions, is shown to be essentially q^2 dependent. The inset plot demonstrates the q independence of the power-law tail exponent of these correlation functions.

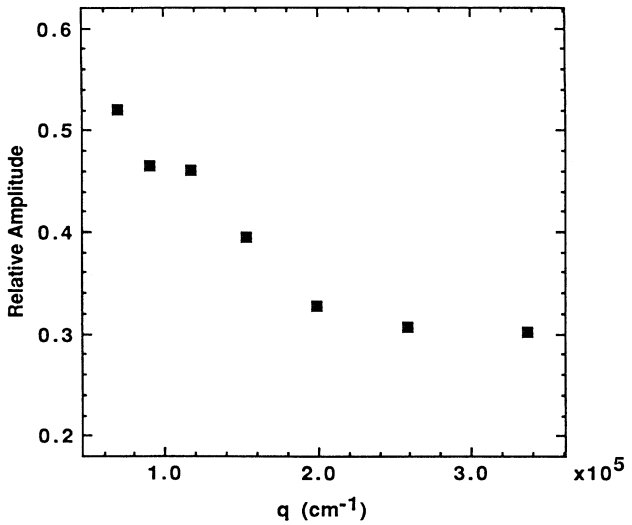

FIG. 11. The relative amplitude A [see Eq. (1)] of the exponential contribution to the gel point correlation function is shown to be dependent on the momentum transfer q. On large length scales the amplitude increases significantly, giving rise to the unusual correlation function shown in Fig. 8.

some sense diffusion dominates the dynamics. In Fig. 9 the relaxation rate Γ is shown to be proportional to q^2, consistent with the interpretation of the initial decay as a cooperative diffusion process with $D_{\text{coop}}=8.3\times10^{-7}$ cm^2/sec. Likewise, the time scale τ associated with the start of the power-law tail, shown in Fig. 10, is also roughly $1/q^2$ dependent, although these data are less convincing since τ is a weaker fitting parameter. Nonetheless, τ is consistently 2–3 times shorter than Γ^{-1} at all q.

The exponent D_p that characterizes the power-law tail is clearly a strong fitting parameter since the tail extends for several decades in time. The data in the inset of Fig. 10 show that this exponent is independent of q, which is certainly a simplifying feature of the data. Finally, Fig. 11 shows that the relative amplitude A of the exponential contribution decreases by a factor of 2 at higher q, where the correlation function assumes the shape of Fig. 7. Thus the pronounced q dependence of the shape of the gel point correlation function is due to the change in the amplitude of the exponential contribution.

C. Beyond the gel point

Beyond the sol-gel transition the curing gel exhibits novel quasielastic scattering properties that are due to the progressive freezing of density fluctuations. This freezing of fluctuations creates difficulties in making scattering measurements, due to the inability to ensemble average in the time domain. In a scattering experiment statistical errors can arise from two sources: finite photon counting and finite fluctuation times. In a laser light scattering experiment photon counting errors are usually negligible since incident intensities are often sufficiently high to run the photon detector up to point where dead-time errors become significant, $\sim10^5$–10^6 Hz (a typical detector dead time is ~100 ns). However, in order to study the relaxation of density fluctuations it is necessary to use a nearly diffraction-limited scattering volume so that the magnitude of the intensity fluctuations is large. If the system has some finite relaxation time τ then the ergodic theorem guarantees that if we signal average for a time $T\gg\tau$ (in practice $T\sim10^4$–$10^6\tau$ is sufficient) we will obtain a correlation function that is independent of the particular scattering volume chosen for the experiment. However, gels pose a particular difficulty, since τ diverges to infinity at the gel point and ergodicity is effectively broken there since T cannot exceed τ.

Beyond the gel point, persistent structural irregularities occur, as evidenced by the grainy appearance of the illuminated volume provided by an impingent laser beam. To describe this phenomena the term "microsyneresis" was coined, syneresis being the exclusion of solvent from a collapsing gel whose elastic contribution to the free energy has created a negative swelling pressure. Thus it was believed that some form of *thermodynamically induced* microphase separation takes place in gels, producing solvent-rich and solvent-poor regimes. Although it is indeed possible that microsyneresis can occur in gels, it is unlikely that the onset of microphase separation would occur at the gel point. Instead, in the case of silica these inhomogeneities appear to be due to the cure-induced freezing of density fluctuations. Beyond the gel point there are many uncondensed hydroxyl groups in a silica gel. Density fluctuations bring these hydroxyl groups together, leading to condensation and a partial pinning of the fluctuation. As this process continues, the gel becomes progressively more heterogeneous. The pinning of fluctuations ultimately leads to a heterogeneous silica gel from which scattering measurements are difficult to make. In fact, elastic light scattering measurements from silica gels[7] produce "noisy" data that are highly scattering volume dependent; a smooth scattering curve is produced only after averaging over many scattering volumes. These problems have also been discussed in the context of the quasielastic light scattering from gels.[15] Finally, it should be mentioned that far beyond the gel point the crosslink density becomes sufficiently high that the elastic free energy finally overcomes the free energy of mixing with the solvent and the silica gel undergoes syneresis.

To study the dynamics beyond the gel point we synthesized a 1M silica gel and collected homodyne autocorrelation functions at a scattering angle of 135° with an argon ion laser operating at $\lambda=457.9$ nm ($1/q=29.7$ nm). The decaying part,

$$S_2(q,t)=[\langle I(0)I(t)\rangle-\langle I(0)I(\infty)\rangle]/\langle I(0)I(\infty)\rangle\ ,$$

of the correlation function taken from a *single* scattering volume at various times beyond the gel point is shown in Fig. 12 for various values of ϵ. Ideally, one should average over many scattering volumes[15] in order to precisely determine the base line $\langle I(0)I(\infty)\rangle$, but in a curing gel it is necessary to make measurements as quickly as possible. This compromise gives rise to the random variations in the shape of the correlation function beyond the gel

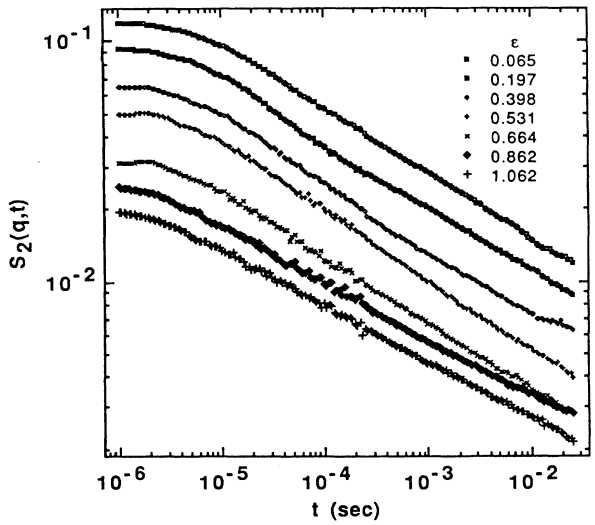

FIG. 12. Correlation functions taken at $q^{-1}=29.7$ nm for a 1M base-catalyzed TMOS gel in the post-gel regime show a decreasing coherent amplitude as the gel modulus increases. However, the power-law decay does not appear to change even long after the gel point. This decrease in the coherent amplitude is accompanied by the appearance of frozen density fluctuations in the gel.

point. Unlike the pre-gel regime, where the shape of $S_2(q,t)$ changes rapidly with time, the shape of the correlation function is essentially unchanged after the gel point, beyond that due to the heterogeneities that naturally arise in silica gels. However, the amplitude of the correlation function decreases substantially with time, just as the elastic shear modulus increases. Data taken long after the gel point ($\sim 5t_{gel}$) show a 45-fold reduction in the amplitude of the coherent signal. Well after the gel point, intensity fluctuations become small and heterogeneities large, so the correlation function starts to depend strongly on the particular scattering volume chosen for study, due to increasing problems with base-line subtraction. In Fig. 13 the initial amplitude of the decaying part of the signal is plotted against ϵ. Empirically, the amplitude appears to decrease exponentially with the time beyond the gel point.

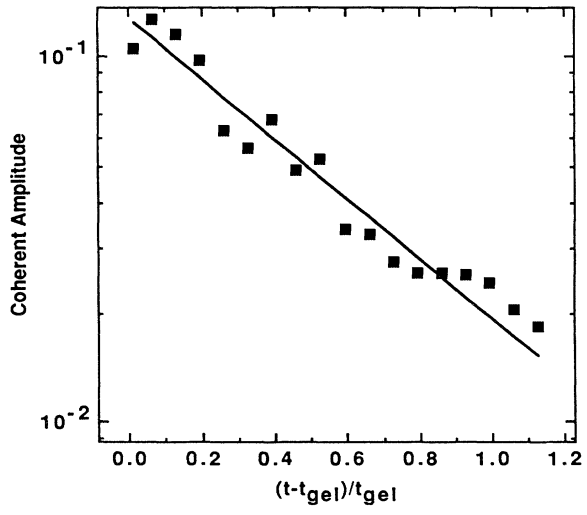

FIG. 13. The initial amplitude of the coherent signal of the correlation functions shown in Fig. 12 is shown to decrease exponentially with time in the post-gel regime. This decrease is a manifestation of the frozen fluctuations observed in silica gels beyond the gel point.

D. Scaling theory of relaxation in gels

At this point it is probably evident to the perspicacious reader that the phenomenology of the relaxation of density fluctuations in gels is complex (or at least not simple). We have observed a stretched exponential tail in $S_2(q,t)$ before the gel point; a power-law decay at and beyond the gel point; the divergence of the time scales $\langle\tau\rangle$ and τ_z while Γ^{-1} does not diverge; and a decrease in the amplitude of the coherent signal beyond the gel point. We have also seen that there appears to be a pronounced cooperative diffusion contribution to the signal at small q.

In order to understand the dynamics it is first necessary to have a structural model of the sol-gel. Near the gel point recent scattering studies of fractal dimensions and radius and mass divergences have shown that the sol-gel transition can be adequately described by the percolation model. This is indeed fortunate, since percolation is also the *only* model of the sol-gel transition. Percolative theories of the viscoelasticity of the incipient gel[4,16] have been successful in describing much of the viscoelastic data on incipient gels, so we will use percolation as the basis of our approach to density fluctuations.

In the simplest cases, the initial decay of a density fluctuation occurs through cooperative diffusion.[17] In cooperative diffusion, the derivative of the osmotic pressure with respect to concentration, $\partial\Pi/\partial c$, provides the restoring force, and the sedimentation coefficient s, due to the viscous flow of the solvent through the incipient network, provides the friction; thus $D_{coop}=s\,\partial\Pi/\partial c$. Since neither of these terms is sensitive to the long-range connectivity that develops at the sol-gel transition, it is reasonable to expect the cooperative diffusion coefficient to vary smoothly throughout the sol-gel transition. As shown in Fig. 6, the initial decay rate is not sensitive to the connectivity divergence, in agreement with this expectation. However, the power-law tail of the gel point correlation function indicates that something extraordinary is contributing to the decay. Physically, a density fluctuation first decays through cooperative diffusion, as the system minimizes its local free energy subject to local constraints. However, if these local constraints decay on a time scale that is long compared to cooperative diffusion, a long-time tail in the correlation function should occur. Thus on large length scales, where the cooperative diffusion relaxation is slow, we see a pronounced exponential contribution to the correlation function, as in Fig. 8.

In semidilute linear polymer solutions, these local constraints are mostly due to entanglements, which give a lo-

cal elastic contribution to the free energy. Modern theories of polymer viscoelasticity are couched in terms of the relaxation of entanglements through translational diffusion, so in macroscopic stress relaxation the importance of entanglements is well accepted. Fluctuations in entanglement density on microscopic length scales will naturally lead to quasiequilibrium states of varying density that relax on the time scale of polymer self-diffusion,[17] a process that may be many orders of magnitude slower than cooperative diffusion; in this indirect fashion self-diffusion couples to the decay of density fluctuations. An "anomalous" slow mode has indeed been observed in semidilute polymer solutions by many investigators,[18,19] and forced Rayleigh scattering measurements[20] have shown that this mode relaxes on approximately the time scale of self-diffusion, yet because a slow mode was unanticipated, these observations are still considered somewhat controversial. However, it is known that the long-time tails in $S(q,t)$ relax more slowly with increasing molecular weight and concentration, as does self-diffusion. In contrast, cooperative diffusion becomes faster with increasing concentration and is independent of molecular weight.

In branched polymer solutions the role of entanglements is not clear, yet the observation of a long-time tail indicates that a single cluster relaxation process may contribute. The relaxation may occur predominately through self-diffusion or it may be due to the relaxation of internal modes of clusters. Our approach is to calculate each of these contributions and compare the results to experimental data.

To understand the dynamics of the incipient gel clusters requires a rudimentary understanding of their percolative structure. The incipient gel is a self-similar distribution of fractal clusters of all sizes, from monomers to the infinite cluster. In order for the distribution of clusters sizes to be self-similar, the average separation distance S between clusters of radius $R \pm d\ln R$ must be proportional to R, so all clusters see the same environment, regardless of their size. Using $S \sim 1/N(R)^{1/d} \sim R$ then gives the power-law *number* distribution $N(R)d\ln R \sim R^{-d} d\ln R$ in terms of the dimension of space d alone. The *hyperscaling* relation[21,22] $N(m)dm \sim m^{-1-d/D} dm$ for the mass distribution can then be obtained from $R^D \sim m$. Thus the cluster size distribution in a branched polymer melt may be regarded as a direct consequence of self-similarity. Slightly beneath the gel point the percolation number distribution is $N(m)dm \sim m^{-1-d/D} e^{-m/M_z} dm$, where the exponential term[21] effectively truncates the distribution at the *typical* cluster mass $M_z \sim \xi^D \sim \epsilon^{-\nu D}$.

1. Cluster self-diffusion

Understanding cluster self-diffusion in the reaction bath is fundamental to understanding the dynamics of branched polymers. Since branched polymers of comparable size cannot overlap it is reasonable to write the self-diffusion coefficient in terms of the Stokes-Einstein relation $D_t = kT/6\pi\eta(R)R$, but in a medium with a *radius-dependent* viscosity (i.e., the microscopic viscosity depends on the cluster size). In other words, we expect the diffusion coefficient of a cluster of radius R to be proportional to that of a sphere of radius R. The radius dependence of the microscopic viscosity can be computed from the following argument. On the time scale in which a cluster of radius R diffuses its own radius, smaller clusters will have diffused a distance much larger than their own radius, or interseparation distance, and will thus be uncorrelated, but larger clusters will remain nearly stationary. Thus to this probe cluster the smaller clusters form a fluid with a finite viscosity, embedded in a tortuous medium of essentially immobile clusters through which the cluster must diffuse. In a self-similar system the tortuosity is the same for all clusters, and merely reduces the diffusion coefficient by some fixed, radius-independent amount. Thus the microscopic viscosity $\eta(R)$ is proportional to the viscosity of a fluid of all clusters of radius $r < R$. Since the cutoff in the power-law size distribution is the correlation length[21] $\xi \sim \epsilon^{-\nu}$, a fluid of viscosity $\eta(R)$ will be observed $\epsilon \sim R^{-1/\nu}$ beneath the gel point, where $\xi \sim \epsilon^{-\nu}$. Noting that the bulk viscosity diverges[22] like $\eta \sim \epsilon^{-k}$ then gives the microscopic viscosity $\eta(R) \sim R^{k/\nu}$, which when combined with the Stokes-Einstein relation $D_t(R) = kT/6\pi\eta R$ gives $D_t(R) \sim 1/R^{1+k/\nu}$ for the diffusion coefficient. In d dimensions this becomes $D_t \sim 1/R^{d-2+k/\nu}$.

The result for the microscopic viscosity can also be obtained by assuming that a probe larger than the correlation length ξ feels the bulk viscosity η_b, and a probe smaller than the correlation length feels a finite viscosity that therefore must be independent of the divergent η_b.[23] This leads to the scaling relation $\eta(R) \sim \eta_b h(R/\xi) \sim \eta_b^0$ for $R < \xi$, and using $\eta_b \sim \xi^{k/\nu}$ then gives $\eta(R) \sim R^{k/\nu}$ for $R < \xi$.

The radius-dependent viscosity is physically due to the screening of hydrodynamic interactions. If hydrodynamic interactions between monomers on a cluster are *completely* screened by smaller clusters in the reaction bath, the Rouse[24] diffusion coefficient $D_t \sim kT/\zeta_0 m \sim 1/R^D$ should apply, where ζ_0 is a monomeric friction factor. Comparing this Rouse expression to $D_t \sim 1/R^{d-2+k/\nu}$ then gives $k = \nu(D-d+2)$ for the viscosity exponent. On the other hand, if hydrodynamic interactions are unscreened, the Zimm[25] diffusion coefficient $D_t \sim 1/R^{d-2}$ leads to $k = 0$. In general, a partial screening of hydrodynamic interactions gives the inequality $0 \le k \le \nu(D-d+2)$. Using the percolation estimate $D \cong (d+2)/2$ yields[4] $0 \le k/\nu \le (6-d)/2$, which demonstrates that in the mean field limit ($d = 6$) k must vanish and the viscosity must diverge at most logarithmically,[22] i.e., $\eta \sim \ln(1/\xi)$. Numerically, experiments should give a viscosity exponent in the range $0 \le k \le 1.35$.

To compute the observed quasielastic light scattering behavior we must recognize that the sol-gel transition is a connectivity divergence, not a thermodynamic phase transition, so there is no singularity in the free energy and no divergent scattering (critical opalescence) from the *undiluted* incipient gel. This implies that the scattering of a single cluster is screened by the other clusters that pack neatly around it. In the absence of monomer-monomer correlations only the diagonal terms in

$S(q)=\sum_{i,j}\langle e^{iq(r_i-r_j)}\rangle$ contribute, so the scattering from a cluster of mass m scales like $S(q)\sim m$, not $S(q)\sim m^2 f(qR)$, where $f(qR)$ is the coherent cluster structure factor. The expression for the self-diffusion contribution to the structure factor is then

$$S_s(q,t)=\int_1^\infty mN(m)e^{-q^2D_t t}dm \ . \tag{2}$$

At zero time this integral is the total mass of the clusters, which does not diverge since mass is conserved. And this integral adequately describes much of the observed dynamics in near-critical gels.

Close to the gel point it is readily shown that the correlation function described in Eq. (1) becomes a power law in time. Using the percolation number distribution $N(m)\sim m^{-1-d/D}e^{-m/M_z}$, along with the relations $D_t\sim 1/R^{1+k/\nu}$ and $D=d-\beta/\nu$, where $G\sim\epsilon^\beta$ is the gel fraction, gives

$$S_s(q,t)\sim t^{-\beta/(\nu+k)}, \quad \Gamma^{-1}<t<\tau_z \tag{3}$$

for the *heterodyne* correlation structure factor at the gel point. The "homodyne" structure factor $S_2(q,t)$ is the square of the heterodyne structure factor, so replacing β by 2β gives the experimentally observed tail. In the Rouse limit the homodyne exponent is $2\beta/(k+\nu)=2d_c/(3-d_c)\cong\frac{2}{5}$ where $d_c\equiv d-D\cong(d-2)/2$ is the codimension of a percolation cluster. In the Zimm limit the homodyne exponent is much larger, with $2\beta/(k+\nu)=2d_c\cong 1$. Thus the Rouse homodyne exponent of $\frac{2}{5}$ is in much better agreement with the experimental value of 0.3. Note that before the gel point the power-law decay is only observed for times greater than Γ^{-1} and smaller than a characteristic time τ_z.

At very long times Eq. (2) predicts a stretched exponential tail before the gel point, as indicated experimentally by the rolloff in the power law in Fig. 4. The method of steepest descents can be used to show that for times exceeding τ_z the correlation function has the stretched exponential tail

$$S_s(q,t)\sim e^{-(t/\tau_z)^{D/(D+1)}}, \quad t\gg\tau_z \ . \tag{4}$$

This tail is due to the exponential truncation of the mass distribution, and is therefore physically due to the diffusion of clusters larger than the correlation length, called lattice animals.[26] These exponentially rare clusters of radius $R\gg\xi$ feel the bulk viscosity η_b and so have a diffusion coefficient $D_t\sim\xi^{-k/\nu}R^{-1}$. The lattice animal fractal dimension of 2 gives a stretched exponential exponent of $\frac{2}{3}$, in good agreement with the data in Fig. 5, which give 0.65 ± 0.5. *A final technical note:* including fluctuations in the steepest descents calculation gives a power-law time prefactor[9] to the stretched exponential decay of Eq. (4). Since this term decays much more slowly than the stretched exponential term it is experimentally irrelevant and so is not included here.

Finally, the divergent time scales observed before the gel point can be calculated directly from Eq. (2). The crossover time $\tau_z=1/q^2D_z$ is the time it takes a typical cluster of radius ξ to diffuse a distance q^{-1}. Using the *z-average* diffusion coefficient $D_z\sim\xi^{-1-k/\nu}$ gives

$$\tau_z\sim 1/q^2D_z\sim\epsilon^{-\nu-k} \ . \tag{5}$$

The Rouse limit $k+\nu=\nu(3-d_c)\cong 2.25$ compares well with the experimental value of 2.5, but the Zimm limit of $k+\nu=\nu\cong 0.9$ is much too small. The arithmetic average relaxation time

$$\langle\tau\rangle\sim\epsilon^{-\nu-k+\beta} \tag{6}$$

is obtained by integrating the heterodyne correlation function. Integrating the homodyne correlation function gives a similar expression, but with β replaced by 2β. The Rouse homodyne exponent is thus $3\nu(1-d_c)\cong 1.35$, to be compared with the experimental value of 1.9, and the Zimm limit gives the quite low value of $\nu+k-2\beta=\nu(1-2d_c)\cong 0$. Finally, the homodyne result $\tau_z/\langle\tau\rangle\sim\epsilon^{-2\beta}$ applies whether or not hydrodynamic interactions are screened, leading to $\beta=0.3\pm0.1$ for the gel fraction exponent, in substantial agreement with the percolation value $\beta=0.39$.

At this point we can conclude that invoking self-diffusion as a mechanism to relieve local constraints, and thus further relax density fluctuations, gives good agreement with the qualitative experimental behaviors, and does a reasonable job of predicting the observed exponents if the Rouse limit is taken. That the Rouse limit should agree well with experiment is not too surprising, since Rouse behavior is also found in viscoelastic measurements.[4]

From another perspective, Eqs. (3)–(6) can be used to determine the gel fraction and viscosity exponents. First define the exponents ϕ and ψ through $S(q,t)\sim t^{-\phi}$ and $\langle\tau\rangle\sim\epsilon^{-\psi}$ and solve the homodyne version of Eqs. (2) and (5) to obtain the expression $\beta=\phi\psi/2(1-\phi)$ for the gel fraction exponent. Using the experimental values $\phi=0.27$ and $\psi=1.9$ then gives $\beta=0.35$, in good agreement with the percolation prediction of $\beta=0.39$. To find k we use the *dilute-solution* experimental value $\nu'=1.35$ for TMOS and correct this for cluster swelling[12] to obtain the reaction bath value $\nu=1.35\times0.8=1.08$. Using $k=\psi-\nu+2\beta$ from Eq. (5) then gives $k=1.5$, in close agreement with the Rouse prediction of $k=1.35$, but in poor agreement with the de Gennes prediction of $k=0.8$, which is based on an analogy between the viscosity divergence and the divergence of conductivity in a superconductor-resistor network.[22] This value of $k=1.5$ is also in good agreement with the viscosity measurements reported recently by Colby *et al.*[27] for base-catalyzed TMOS sol-gels, which gave $k=1.3$. Finally, substituting these exponents into Eq. (4) gives $\tau_z\sim\epsilon^{-2.6}$, in good agreement with our experimental observation $\tau_z\sim\epsilon^{-2.5\pm0.1}$.

2. *Cluster configurational diffusion*

That cluster self-diffusion is so successful in explaining the long-time relaxation of density fluctuations in silica gels may be due to the local rigidity of these colloidal gels. In more flexible systems, where the persistence

length is much smaller than q^{-1}, it is possible that constraints on density fluctuations may instead be relieved through the internal relaxations of clusters. If the idea of the single cluster scattering being screened is again invoked, the relaxation of density fluctuations is described by Eq. (1) with $\exp(-q^2Dt)$ replaced by a sum over normal modes. However, this substitution results in a form that is the basis of viscoelastic theories[4] of gels. *A priori,* this correspondence seems reasonable since the analogy between the dynamics probed by quasielastic light scattering and viscoelasticity is strong when cluster overlap leads to screening of the scattered field. However, although the analogies between light scattering and viscoelasticity are interesting, the agreement with experimental data makes this connection unconvincing.

In the following we describe the correspondence between viscoelasticity and quasielastic light scattering in the Rouse limit. The power-law tail of the heterodyne correlation function corresponds to the stress relaxation modulus[4] $G(t)\sim t^{-d/(2+D)}\sim t^{-2/3}$. Viscoelastic data for TMOS gels give $G(t)\sim t^{-0.55\pm0.05}$ in substantial agreement with this prediction. However, this viscoelastic exponent is more than twice the heterodyne scattering exponent of 0.25 observed in polyurethane gels,[28] a flexible system, and is much larger than the self-diffusion exponent of $d_c/(3-d_c)\cong 0.2$. The average relaxation time $\langle\tau\rangle$ is analogous to the viscosity,[4] which diverges like $\eta_b\sim\epsilon^{-\nu(2-d_c)}\sim\epsilon^{-1.35}$, in contrast to the translational diffusion model prediction of $\langle\tau\rangle\sim\epsilon^{-1.8}$. The measured polyurethane divergence is only $\langle\tau\rangle\sim\epsilon^{-1.1}$. Finally, in the viscoelasticity theory the longest characteristic time[4] τ_z is the product $\eta_b J_e^0\sim\epsilon^{-\nu(d+2-d_c)}\sim\epsilon^{-4}$, where J_e^0 is the equilibrium steady-state creep compliance. This is much stronger than the self-diffusion divergence $\tau_z\sim\epsilon^{-\nu(3-dc)}\sim\epsilon^{-2.5}$. Thus we see that although there are strong analogies between the dynamics observed in light scattering and that observed in linear viscoelasticity, the measured exponents are in better agreement with the self-diffusion description.

IV. BRANCHED POLYMER SOLUTIONS

A. Light scattering measurements

Light scattering measurements from dilute linear polymer solutions have allowed the investigation of a number of interesting single polymer properties, such as translational diffusion and the relaxation of internal modes. In this section we explore the scattering behavior of branched polymers that are diluted at the gel point, in an effort to understand how the power-law tail of the correlation function changes upon dilution. Because the optical screening arguments that were applied to the reaction bath do not hold in dilute solutions, we expect to observe dramatic changes in the dynamics. In particular, $S(q,t)$ should be integrable in dilute solutions, so that it is possible to observe "critical slowing down" by approaching the gel point along the concentration axis.

When the reaction bath is diluted two effects occur: individual branched polymers separate, leading to a dramatic increase in the scattered intensity per unit concentration; and the branched polymers swell because two-body, monomer-monomer interactions are no longer screened as in the reaction bath.[29–31] The net effect of dilution is to significantly increase the spatial correlation length[32] ξ_s over its reaction bath value of $\xi_0\sim 10$ nm. Static light scattering experiments[33] show that upon dilution from the reaction bath concentration of C_0 this spatial correlation length increases as $\xi_s\cong\xi_0(C_0/C)^2$ until the solution is sufficiently dilute that ξ_s becomes the z-average cluster radius. On length scales $q\xi_s\gg 1$ only intermediate scattering is observed, and this decays as $I\sim q^{-D_e}$ where $D_e=D(3-\tau)\cong 1.6$ is the ensemble fractal dimension.[34]

The appearance of a significant correlation length in semidilute solutions can be seen in Fig. 14, where scattering data are shown for a $1M$ base-catalyzed TMOS sol-gel diluted at the gel point. Although light scattering from the undiluted sample revealed essentially no q dependence (not shown), even a moderate, 1.5-fold dilution yields a significant scattering dissymmetry. At the lowest concentrations the intermediate scattering $I\sim q^{-1.6}$ is observed, indicating sufficiently large clusters (larger than ~ 1000 nm) that $q\xi_s\gg 1$ in the light scattering q window. The extraordinary concomitant changes in the dynamics of density fluctuations are unforeshadowed by the simple concentration dependence of the static scattering of the critical gel, as we shall now discuss.

When a critical sol-gel is diluted by a factor of 1.5, the

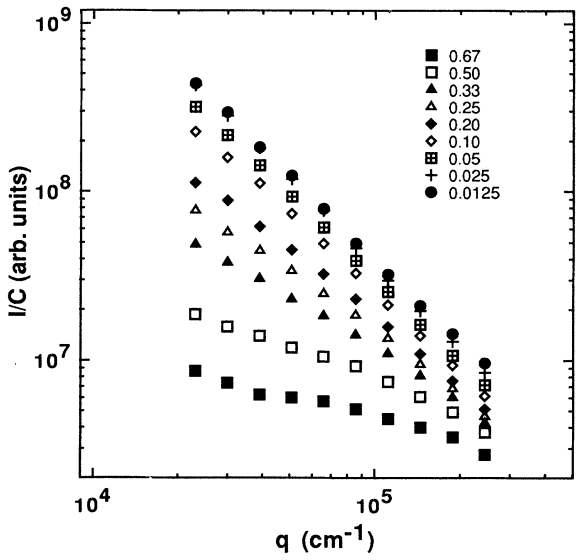

FIG. 14. The intensity of scattered light per unit concentration of silica is shown to increase with dilution, due to the swelling of clusters and the elimination of optical screening increasing the spatial correlation length. These measurements were made by bringing a $1.0M$ TMOS sol-gel to the gel point and diluting the branched polymers thus formed with methanol. At the lowest concentrations the scattering is in the intermediate regime, where $qR_z\gg 1$, and shows fractal scaling with $I\sim q^{-1.6}$. Thus the ensemble fractal dimension is 1.6. These data are consistent with a power-law increase $\xi_s\cong\xi_0(C_0/C)^2$ in the spatial correlation length.

long-time tail of the intensity autocorrelation function changes from a power law to a stretched exponential decay, as shown in Fig. 15. The static scattering data indicate that $q\xi_s \ll 1$ in this case, however, upon further dilution the spatial correlation length becomes very large, till eventually $q\xi_s \gg 1$. In this case the stretched exponential decay gradually crosses over to a more rapid decay that has no readily discernible functional form, as shown in the top curve in Fig. 15. Thus as the system is diluted the relaxations become progressively more rapid, indicating that the critical slowing down that is observed in the reaction bath can also be approached along the concentration axis. In fact, integration of the homodyne autocorrelation functions, Fig. 16, demonstrates a strongly divergent average relaxation time $\langle\tau\rangle \sim (C_0 - C)^{-5.9}$ as C approaches the reaction bath concentration C_0.

Studies of the q dependence of the dynamic structure factor of diluted critical gels reveal two time scales that depend on different powers of the momentum transfer. Autocorrelation functions for the 1.5-fold diluted sol taken at different values of q are shown in Fig. 17 on the dimensionless axis $(\Gamma t)^{0.24}$, where Γ is the initial decay rate. These correlation functions do not collapse at long times on this dimensionless axis because the characteristic time for the tail is not proportional to Γ^{-1}. In fact, the initial decay rate is q^2 dependent, indicating a decay dominated by cooperative diffusion, whereas the stretched exponential tail $\exp[-(t/\tau)^{0.24}]$ has a relaxation rate τ^{-1} that is $q^{3.3}$ dependent. The crossover between these regimes is surprisingly abrupt.

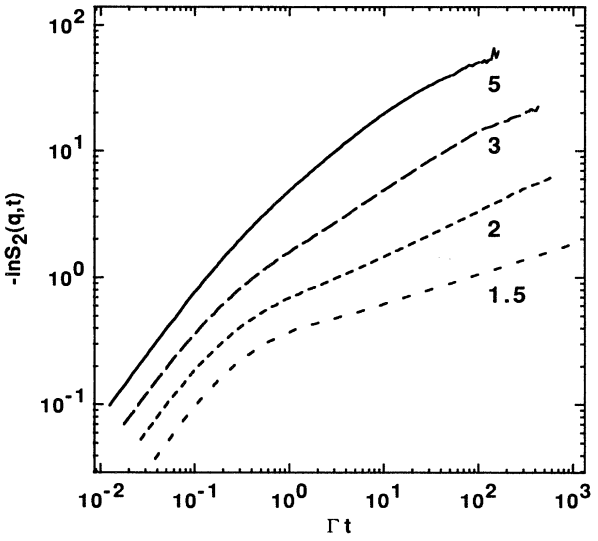

FIG. 15. Homodyne intensity autocorrelation functions for diluted TMOS critical gels show a sensitive dependence on concentration (the dilutions are the numbers beneath each curve). These data were taken at a scattering angle of 135° with a He-Ne laser at $\lambda = 632$ nm ($q = 243\,300$ cm^{-1}) and Γ is the first cumulant. On this log-log vs log plot, a stretched exponential decay $\exp[-(t/\tau)^b]$ is a straight line with a slope of b. At a dilution of 1.5 the correlation function shows the expected exponential slope of $b = 1$ at early times, but then crosses over to a slope of $b = 0.24$ at large times, obtained from a nonlinear least squares fit to the data. Likewise, the two-fold dilution gives $b = 0.38$ and the three-fold dilution gives $b = 0.46$. As the branched polymers are further diluted, the stretched exponential decay crosses over to a much more rapid decay that appears to have no simple functional form, but can be attributed to the internal modes of the clusters.

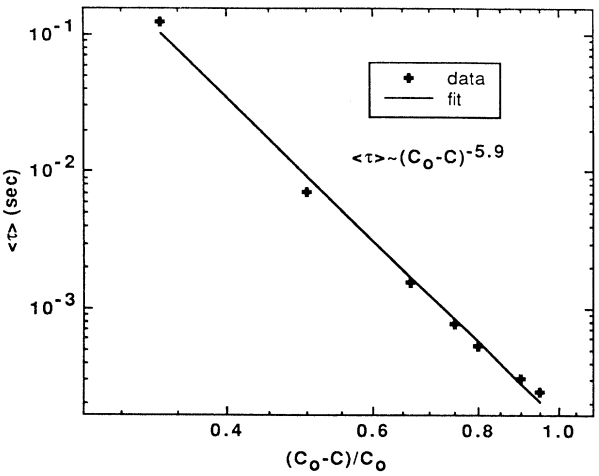

FIG. 16. The critical slowing down in the reaction bath at t_{gel} is usually approached along the time (extent of reaction) axis, as in Fig. 6. However, these data show that it is also possible to observe critical slowing down by approaching this critical condition along the concentration axis. These data were obtained by diluting a critical sol-gel and integrating homodyne correlation functions taken at $q = 243\,300$ cm^{-1}. At the highest concentration it was necessary to integrate the tail analytically from the stretched exponential curve fit to prevent truncation errors. These data also strongly suggest that in a dilute solution the divergence occurs at the reaction bath concentration C_0.

At much higher dilutions the stretched exponential correlation function with two time scales crosses over to a more rapidly decaying form with a single $\sim q^3$ dependent decay rate, as shown for 80-fold diluted gels in Fig. 18. Integration of these correlation functions gives a single time scale $\Gamma \sim q^{2.76}$. Since the measurements are in the intermediate scattering regime $q\xi_s \gg 1$, it is reasonable to assume we are observing the internal modes of branched polymers in this case. Correlation functions taken at intermediate values of dilution showed a crossover between the slow, stretched exponential behavior of the 1.5-fold diluted gels and the rapid decay of the 80-fold diluted gels. For example, the two-fold diluted gel gave a stretched exponential exponent of 0.38, the three-fold sample gave 0.46, the five-fold sample gave 0.54, and the ten-fold sample showed no real stretched exponential regime. The interpretation of these results is still incomplete, but it is still possible to draw some conclusions about the flexibility of the clusters from these measurements.

B. Translational diffusion

1. Power-law decay

In the most dilute branched polymer solutions translational diffusion alone dominates the decay of the correla-

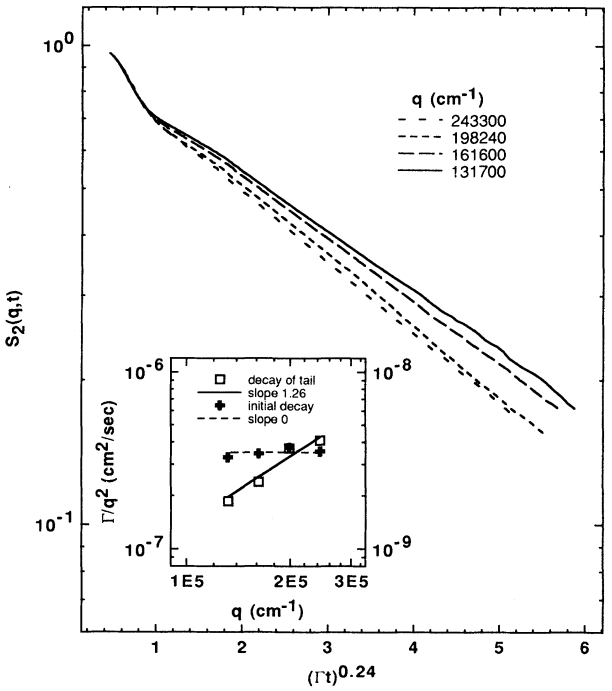

FIG. 17. Homodyne correlation functions taken for a 1.5-fold diluted critical silica sol-gel show a stretched exponential decay at long times for all values of the momentum transfer q. However, when plotted against the dimensionless time Γt, where Γ is the initial decay rate, the long-time tails do not collapse, indicating the presence of two time scales in the correlation functions. The inset graph demonstrates this point: the initial decay rate is proportional to q^2, but the decay rate $1/\tau$ of the tail is proportional to q^3. The q^2 dependence is consistent with cooperative diffusion, but the q^3 dependence is indicative of a decay process that occurs in the absence of an identifiable length scale.

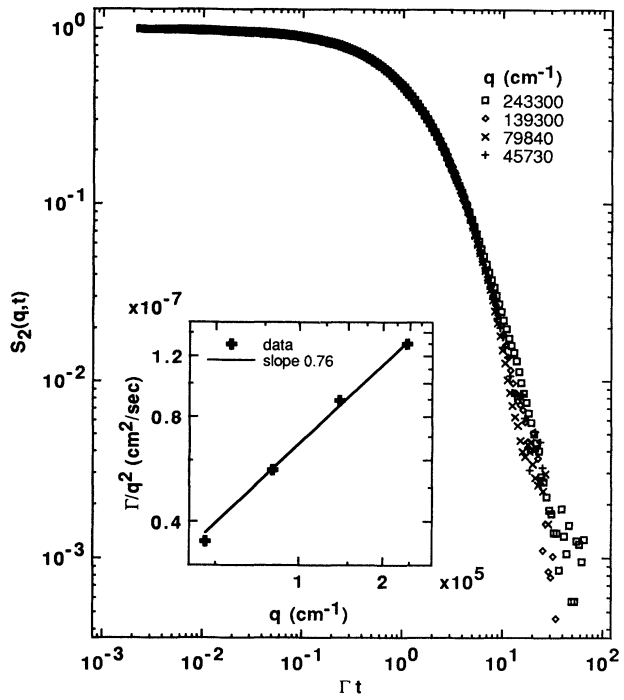

FIG. 18. Critical sol-gels diluted 80-fold are essentially dilute in the light scattering window since the scattered intensity is purely intermediate. For these dilute branched polymers both the initial decay rate $\Gamma=\langle 1/\tau\rangle$ and inverse decay time $1/\langle\tau\rangle$ scale as $q^{2.76}$, so the correlation functions are described by a single time scale and collapse to a master curve on nondimensioned axes. The long-time decay of these homodyne correlation functions is probably due to the complex normal modes of branched polymers.

tion function if the condition $q\xi_s \ll 1$ is satisfied. However, our experiments at low concentration were made in the $q\xi_s \gg 1$ regime where internal cluster deformation modes must contribute to the observed decay, provided the clusters are flexible. In a dilute solution of branched polymers the translational diffusion of the power-law polydisperse clusters can give the experimental observation $\Gamma \sim q^3$ in the $q\xi_s \gg 1$ regime, so it is worthwhile to determine whether the *shape* of the correlation functions can also be described by translational diffusion alone before we consider the effect of internal modes.

For a dilute solution of rigid clusters with negligible form anisotropy, the unnormalized dynamic structure factor is[35]

$$S(q,t)=\int_0^\infty m^2 S_m(q) N(m) e^{-q^2 D t} dm \ , \tag{7}$$

where $S_m(q)$ is the static structure factor normalized such that $S_m(0)=1$. Since the fractal dimension of a swollen branched polymer is 2, it is sufficient to approximate $S_m(q)$ by the Ornstein-Zernike function $1/(1+q^2R^2)$ where R is the cluster radius (the detailed choice does not affect our result). If we are interested only in the intermediate scattering limit where $qR_z \gg 1$, then it is sufficient to use the gel point polydispersity, $N(m)\sim 1/m^\tau$. Changing variables to remove the integrable singularity at the origin then gives the unnormalized form

$$S(\Omega t)=\int_0^\infty \frac{1}{1+x^{1/(\tau-2)}} e^{-\Omega t x^{1/2(\tau-2)}} dx \ , \tag{8}$$

where $\Omega t = q^3 t kT/6\pi\eta_0$ is a dimensionless time and η_0 is the solvent viscosity. It can be shown that the short-time decay of Eq. (8) is exponential with a first cumulant[35] $\Gamma \sim \Omega \sim q^3$, in accord with our observations on dilute solutions. However, for $\Gamma t > 1$ the heterodyne correlation function exhibits the power-law decay

$$S(q,t) \sim \frac{1}{(\Gamma t)^{2(\tau-2)}} \ . \tag{9}$$

Using $\tau = 1 + d/D$ gives a homodyne exponent of $4d_c/D \cong 0.8$, which is a much slower decay than is observed experimentally. In fact, the correlation functions in Fig. 18 do not appear to be power laws at all, but if one were to force-fit the long-time tail to a power law, an exponent of about 2 would be obtained. Thus it is clear that translational diffusion alone cannot account for the decay observed in solution, indicating that the swollen

clusters have some flexibility on light scattering length scales.

2. *Stretched exponential decay*

In general, if the system is slightly beneath the gel point then at very large times the exponentially large clusters will dominate the decay provided that these clusters are sufficiently rigid that normal modes do not contribute to the observed relaxations. In this case the stretched exponential decay of Eq. (4) applies, but with the solvent viscosity η_0 incorporated into the terminal time τ_z.

C. Internal modes

The contribution of internal modes to the dynamic structure factor of linear polymers in dilute solution is reasonably well understood, and serves as a useful reference point for branched polymers. Detailed calculations[36,37] show that on length scales large compared to the polymer radius the decay is due to translational diffusion, and that on intermediate length scales $qR > 1 > qa$ (a is the persistence length of the polymer) the decay is dominated by the relaxation of internal modes, which is much more rapid than the translational diffusion contribution. In fact, in the intermediate regime the initial relaxation time is just the time Ω^{-1} it would take a cluster of radius q^{-1} to diffuse a distance q^{-1}. In the Zimm limit[17] the initial relaxation rate is

$$\Gamma = \frac{\Omega}{u} f(u) , \tag{10}$$

where $u = qR$ and $\Omega = q^3 kT/6\pi\eta_0$. The function $f(u) = 1$ in the translational diffusion dominated regime $u \ll 1$, yielding $\Gamma = q^2 D_t$, and $f(u) \sim u$ in the internal mode dominated regime $u \gg 1$, giving the radius-independent relaxation rate $\Gamma \sim q^3 kT/6\pi\eta_0$. Since this scaling of the initial relaxation rate is quite general, relying only on the absence of an internal length scale and hydrodynamic interactions, Eq. (10) should hold for flexible *branched* polymers as well.

The functional form of the time decay of $S(q,t)$ is also dependent on the scattering length scale. In the translational diffusion regime the decay is a single exponential, but internal modes from *Gaussian* polymers with hydrodynamic interactions give the stretched exponential decay[37]

$$S(q,t) \sim e^{-(\Omega t)^{2/3}} , \tag{11}$$

where $\Omega = q^3 kT/6\pi\eta_0$. (This should not be confused with the stretched exponential decay that results from the translational diffusion of rigid, exponentially rare lattice animals.) A diffusive and internal mode regime should also be found in QELS measurements from monodisperse solutions of branched polymers, and it is reasonable to expect the form of the correlation function in the internal mode regime to be the stretched exponential of Eq. (11), but this would be quite difficult to prove with any degree of rigor.

The interpretation of dynamic data from branched polymer solutions is further complicated by the fact that in the intermediate scattering regime where $qR_z \gg 1$ there are always small clusters for which $qR \ll 1$ and large clusters for which $qR \gg 1$. Thus the small clusters contribute to the observed relaxation through translational diffusion and the large clusters contribute through the relaxation of internal modes. This polydispersity dominates the dynamics, giving the power-law decay in Eq. (9), if internal modes are neglected, but if internal modes are included the large time decay is dominated by internal modes and is *independent* of polydispersity.

The combined effects of polydispersity and internal modes can be expressed by rewriting Eq. (7) in the more general form

$$S(q,t) = \int_0^\infty \frac{u^{D(3-\tau)}}{(1+u^2)^{D/2}} S(u,\Omega t) \frac{1}{u} du . \tag{12}$$

Here D is the fractal dimension of a diluted cluster, $S(u,\Omega t)$ is the single cluster dynamic structure factor, normalized such that $S(0,0) = 1$, and $u = qR$. For a flexible self-similar cluster, we expect $S(u,\Omega t)$ to have two limiting behaviors; the diffusive limit $S(u,\Omega t) = e^{-\Omega t/u}$ for $u < 1$, and the internal mode limit $S(u,\Omega t) = e^{-f(\Omega t)}$ for $u > 1$. Note that the characteristic time u/Ω depends on the length scale R in the diffusive limit, whereas the internal mode time scale Ω is independent of R. By splitting the interval of integration into $[0,1]+[1,\infty]$ it can then be shown that the diffusive part is dominated by an exponential decay at large times. The internal mode contribution, however, is then

$$\int_1^\infty \frac{e^{-f(\Omega t)}}{u^{D(\tau-2)}} \frac{1}{u} du \sim e^{-f(\Omega t)} . \tag{13}$$

If this decay is slower than exponential, as it is in linear polymers, then this term will dominate the diffusive term at long times. In this case the gel point polydispersity has no effect on the time dependence of intermediate scattering from flexible clusters at long times and *the long-time tail of the correlation function is just the single cluster relaxation function.* This is in contrast to the q dependence of the intermediate scattering, which is strongly affected by the polydispersity. Physically, this result implies that at early times the decay is dominated by the translational diffusion of the self-similar distribution of small clusters. After clusters satisfying $qR \ll 1$ relax in this fashion, the larger clusters provide a relaxation via internal modes that is independent of their radius, being roughly the time Ω^{-1} it takes a cluster of radius q^{-1} to diffuse a distance q^{-1}. It is most reasonable to expect this long-time tail to be the stretched exponential in Eq. (11), but experiments indicate that the long-time tail has no simple form, so it remains a challenging theoretical problem to compute the dynamic structure factor for a branched polymer in a good solvent with hydrodynamic interactions.

It is clear that solutions of branched polymers provide some of the most vexing theoretical issues. Our measurements indicate that the power law observed at the gel point crosses over to a stretched exponential decay characterized by two distinct regimes at moderate dilution. In dilute solution the correlation functions can be

described by a single time scale that depends on $1/q^{2.8}$, strongly suggestive of internal modes. We have shown that a time scale of $1/q^3$ is expected, and that the long-time tail of the correlation function is unaffected by the self-similar size distribution of the branched polymers.

V. CONCLUSIONS

In this paper we have undertaken an exhaustive experimental investigation of the relaxation of density fluctuations in gelling systems, including studies in the reaction bath, and of semidilute and dilute solutions of branched polymers. In the reaction bath a novel critical dynamics is observed that is characterized by a power-law spectrum of relaxation times at the gel point with a longest time that diverges at $t_{\rm gel}$. This spectrum is experimentally observed in the power-law relaxation of the dynamic structure factor and in the divergence of two characteristic time scales. A simple cluster diffusion model of the dynamics is proposed that relies on the concept of a size-dependent viscosity, the hyperscaling form of the size distribution, and the screening of the scattered intensity. This cluster diffusion interpretation accounts for the power-law time decay of $S(q,t)$ at the gel point, the divergence of the average and longest relaxation times, and the stretched exponential decay before the gel point.

Beyond the gel point the gel becomes effectively nonergodic and the magnitude of fluctuations decreases dramatically with the extent of reaction. The nonergodicity is manifested in the inability to obtain a smooth scattering function from a single scattering volume. Curiously, the power-law decay of $S(q,t)$ continues after the gel point, although the small amplitude of the correlated signal beyond the gel point makes measurements of this power law progressively more difficult.

Studies of semidilute solutions of branched polymers show a stretched exponential time decay characterized by the presence of multiple time scales, including an early time decay with a decay rate proportional to q^2 and a late time decay rate proportional to $q^{3.3}$. Dilute solutions do not show a stretched exponential decay, and are described by a single decay rate proportional to $q^{2.8}$, and it is possible to show that the long-time decay in polydisperse solutions is just the *monodisperse* decay. Understanding this decay will require a detailed theory of the relaxation of normal modes in branched polymers. Finally, the divergence of the average relaxation time along the concentration axis is much stronger than the divergence along the time axis.

It should by now be evident that even a rough characterization of the decay of concentration fluctuations near the sol-gel transition produces a wealth of unusual findings. These observations should vex the minds of theoreticians for years to come, and should provide a growth industry for experimentalists as well, as the universality of these findings is explored.

ACKNOWLEDGMENTS

This work was performed under the auspices of the U.S. Department of Energy and funded in part by its Office of Basic Energy Sciences, Division of Materials Sciences, under Contract No. DE-AC04-76DP00789.

[1]J. E. Martin and J. P. Wilcoxon, Phys. Rev. Lett. **61**, 373 (1988).
[2]M. Adam, M. Delsanti, and J. P. Munch, Phys. Rev. Lett. **61**, 706 (1988).
[3]F. Chambon and H. H. Winter, Polym. Bull. **13**, 499 (1985); H. H. Winter, P. Morganelli and R. Chambon, Macromolecules **21**, 532 (1988).
[4]J. E. Martin, D. Adolf, and J. P. Wilcoxon, Phys. Rev. Lett. **61**, 2620 (1988); Phys. Rev. A **39**, 1325 (1989).
[5]D. Durand, M. Delsanti, M. Adam, and J. M. Luck, Europhys. Lett. **3**, 297 (1987).
[6]B. J. Berne aand R. Pecora, *Dynamic Light Scattering* (Wiley, New York, 1976).
[7]J. E. Martin and J. P. Wilcoxon, Phys. Rev. A **39**, 252 (1989).
[8]P. Meakin, *Phase Transitions* (Academic, New York, 1988), Vol. 12, p. 336.
[9]J. E. Martin, Phys. Rev. A **36**, 3415 (1987).
[10]J. E. Martin, J. P. Wilcoxon, and J. Odinek (unpublished).
[11]P. Meakin and M. Muthukumar, J. Chem. Phys. **91**, 3212 (1989).
[12]J. E. Martin, J. P. Wilcoxon, and D. Adolf, Phys. Rev. A **36**, 1803 (1987).
[13]H. L. Swinney and D. L. Henry, Phys. Rev. A **8**, 2586 (1973).
[14]B. B. Mandelbrot, *The Fractal Geometry of Nature* (Freeman, New York, 1983), p. 247.
[15]P. N. Pusey and W. van Megen, Physica A **157**, 705 (1989).
[16]M. Muthukumar, J. Chem. Phys. **83**, 3161 (1985); M. E. Cates, J. Phys. (Paris) **46**, 1059 (1985).
[17]P. G. de Gennes, *Scaling Concepts in Polymer Physics* (Cornell, New York, 1979), p. 216.
[18]E. J. Amis and C. C. Han, Polymer **23**, 1403 (1982); E. J. Amis, P. A. Janmey, J. D. Ferry, and H. Yu, Macromolecules **16**, 441 (1983); E. J. Amis, C. C. Han, and Y. Matsushita, Polymer **25**, 650 (1984).
[19]W. Brown, R. M. Johnsen, and P. Stilbs, Polym. Bull. **9**, 305 (1983); W. Brown, Polymer **25**, 680 (1984); W. Brown, Macromolecules **17**, 66 (1984).
[20]T. Chang and H. Yu, Macromolecules (to be published).
[21]D. Stauffer, *Introduction to Percolation Theory* (Taylor and Francis, London, 1985).
[22]D. Stauffer, A. Coniglio, and M. Adam, in *Advances in Polymer Science 44,* edited by K. Dušek (Springer-Verlag, Berlin, 1982).
[23]P. G. de Gennes, J. Phys. Lett. (Paris) **40**, L197 (1979).
[24]P. E. Rouse, J. Chem. Phys. **21**, 1272 (1953).
[25]B. H. Zimm, J. Chem. Phys. **24**, 269 (1956).
[26]H. E. Stanley, P. J. Reynolds, S. Redner, and F. Family, in *Real-Space Renormalization,* edited by T. W. Burkhardt and J. M. J. van Leeuwen (Springer Verlag, Heidelberg, 1982).
[27]R. H. Colby, B. K. Coltrain, J. M. Salva, and S. M. Melpolder, in *Fractal Aspects of Materials: Disordered Systems,* edited by A. J. Hurd, D. A. Weitz, and B. B. Mandelbrot, (Materials Research Society, Pittsburgh, 1987).
[28]M. Adam, M. Delsanti, and J. P. Munch, Phys. Rev. Lett. **61**,

706 (1988).
[29]J. Isaacson and T. C. Lubensky, J. Phys. (Paris) **41**, L469 (1980).
[30]P.-G. de Gennes, C. R. Acad. Sci. Paris **291**, 17 (1980).
[31]M. Daoud, F. Family, and G. Jannink, J. Phys. (Paris) Lett. **45**, 199 (1984).
[32]M. Daoud and L. Leibler, Macromolecules **21**, 1497 (1988).
[33]J. E. Martin and J. Odinek, Macromolecules **23**, 3362 (1990).
[34]J. E. Martin and K. D. Keefer, Phys. Rev. A **34**, 4988 (1986); E. Bouchaud, M. Delsanti, M. Adam, M. Daoud, and D. Durand, J. Phys. (Paris) **47**, 1273 (1986).
[35]J. E. Martin and B. J. Ackerson, Phys. Rev. A **31**, 1180 (1985); J. E. Martin and F. Leyvraz, *ibid.* **34**, 2346 (1986).
[36]P.-G. de Gennes, Physics **3**, 37 (1967).
[37]E. Dubois-Violette and P.-G. de Gennes, Physics **3**, 181 (1967).